Effect of operating conditions on the retention of ruthenium tetroxide (RuO4) by different solid traps

Thibault Bagnol, Julie Nguyen-Sadassivame, Marie Noelle Ohnet, B. Azambre, Christophe Volkringer, Thierry Loiseau, Laurent Cantrel, Philippe Nerisson

Effect of operating conditions on the retention of ruthenium tetroxide (RuO_4) by different solid traps

Thibault Bagnol[1], Julie Nguyen-Sadassivame[1,2], Marie-Noëlle Ohnet[1], Bruno Azambre[3], Christophe Volkringer[2], Thierry Loiseau[2], Laurent Cantrel[1], Philippe Nerisson[1*]

[1] Institut de Radioprotection et de Sûreté Nucléaire, PSN-RES/SEREX/L2EC, BP 3, 13115 Saint-Paul-Lez-Durance Cedex, France

[2]Université de Lille, CNRS, Centrale Lille, Univ. Artois, UMR 8181 - UCCS - Unité de Catalyse et Chimie du Solide, F-59000 Lille, France

[3]Université de Lorraine, Laboratoire de Chimie et de Physique - Approche Multi-échelles des Milieux Complexes (LCP-A2MC), Rue Victor Demange, 57500 Saint-Avold, France

*Corresponding author: philippe.nerisson@irsn.fr

ABSTRACT

Mitigation of gaseous RuO_4 is an important issue in nuclear safety in order to reduce potential radiological consequences, either in the context of severe accident arising on pressurized water reactors (oxidizing conditions) or in reprocessing plants (loss of cooling of fission product storage tanks). For the first time, RuO_4 trapping was compared using three kinds of materials acting as solid traps: a functionalized MOF UiO-66-NH_2, an amine-modified silica and a commercial cerium dioxide. Different experimental conditions of temperature, humidity and gas composition were investigated in order to mimic those prevailing under accident conditions at filtered containment venting system (FCVS) level or in ventilation ducts (gas mixture). At 50 °C, the efficiency of UiO-66-NH_2 for RuO_4 trapping was both very high in dry gas and in presence of steam with decontamination factor (DF) in the range 10^4-10^5. Under more severe conditions, the retention performances slightly decrease, especially when NO_2 was present in the feed gas due to some poisoning of adsorption sites. In presence of amino-modified silica, breakthrough of RuO_4(g) occurred at an earlier stage due to its inferior adsorption capacity but the performances of the trap did not deteriorate in presence of steam and NO_2 in gas mixture. Under similar conditions, cerium dioxide showed no retention of RuO_4(g).

KEYWORDS: ruthenium tetroxide mitigation, Metal-Organic Framework, gas-solid adsorption

1. INTRODUCTION

Ruthenium is a fission product generated in nuclear power plants from (NPP) uranium oxides used as nuclear fuel. In various accidental scenarios, the mitigation by filtration of gaseous ruthenium tetroxide (RuO_4) releases remains an important issue due to its radiotoxicity and its ability to disperse radioactivity to the environment [1]. Indeed, RuO_4 outside releases could occur in the context of a severe accident in pressurized water reactor (PWR) in very oxidizing conditions ([2]-[7]), as well as in reprocessing plants ([8]-[12]) or other nuclear facilities.

From a general viewpoint, the capture of RuO_4 has received much less attention than that of volatile iodine species. Nevertheless, some recent works have been focused on RuO_4 trapping in FCVS (Filtered Containment Venting System). These devices are part of some nuclear building containment in nuclear power plants. Two types of FCVS can be distinguished. In “wet” FCVS, the filtration module consists in scrubbers containing alkaline solution and is able to trap RuO_4(g) by “pool scrubbing” with conversion into ruthenates (RuO_4^{2-}) and perruthenates (RuO_4^-) ions [13]. The second category corresponds to “dry” FCVS, such a metallic prefilter and/or a sand bed filter, not able to trap RuO_4 [14].

In reprocessing fuel context, the issue of ruthenium behaviour in nitric media (HLLW: High Level Liquid Wastes) has started to be studied since the 80's. However, the need of re-assessing the knowledge on this topic, notably RuO_4 mitigation, has been deeply reconsidered after the Fukushima-Daiichi NPP accident ([15]-[20]).

Recently, many solid adsorbents were investigated by us and others for the trapping of various radiospecies, including RuO_4.

- Metal-Organic Frameworks (MOFs) materials, corresponding to hybrid porous solids composed of a variety of organic ligands and metallic cluster (Zn, Al, Cu, Zr, etc) [21]. Thanks to their high porosity and specific surfaces (up to 7000 m^2/g), these materials are used in gas sorption, catalysis or drug release [22]. In the nuclear domain, MOF compounds have shown different interests, notably:
    - some efficiency for the capture of various radionuclides in liquid solutions [23] [24],
    - an ability to act as solid traps in gaseous fission products mitigation, especially iodine [25][27] and ruthenium. In that respect, it has been demonstrated that MOF UiO-66-NH_2 presents very good capacities for RuO_4 trapping in dynamic and smooth operating conditions (T, RH) [25][28].
- Organo-modified silica with (poly)amine groups such as polyethylene imine (PEI): such compounds have already been reported and optimized for carbon dioxide capture [29]. More recently, they have been studied for gaseous fission products mitigation such as I_2 with a very high adsorption capacity up to ~ 2 g/g at 100 °C [30], or ruthenium tetroxide [17] in smooth conditions.
- Rare earth oxides: CeO_2 based materials are well known in automotive catalysis and other applications for their oxygen storage capacity (OSC) associated with the easy switch between the Ce +III and +IV oxidation state. Their main interests in this context are their redox character as well as their thermal stability. Cerium dioxide based materials were recently studied for ruthenium tetroxide mitigation and showed some interest when doped with Zr in smooth conditions due to their reducing ability [17].
- Zeolites or active charcoals, well known for iodine trapping [31][32], have shown no retention of RuO_4(g) in smooth conditions [17].

This study aims at continuing the experimental study carried out with zirconium-based MOF UiO-66-NH_2 compound for RuO_4 trapping [28], by testing conditions representative of those occurring in the FCVS during severe nuclear accident or as in ventilation ducts in reprocessing plants. Hence, the effects of parameters such as temperature, humidity and presence of nitrogen oxides were studied both alone or in combination. Besides, the performances of MOF for RuO_4 retention are compared with other solid compounds such as a commercial silica modified with PolyEthylene Imine (PEI) and a commercial rare earth oxide CeO_2.

2. MATERIALS AND METHODS

2.1. Experimental device: SAFARI

The experimental device called SAFARI (meaSurement of filtrAtion eFficiency of mAterial with regard to Ruthenium or Iodine) has been designed to determine the decontamination factor of an adsorbent bed with respect to gaseous ruthenium tetroxide [25][28]. On Figure 1 is displayed a scheme of SAFARI test bench. It is constituted of three parts: ruthenium tetroxide generation, ruthenium tetroxide mitigation and ruthenium tetroxide trapping in solution [14][28].

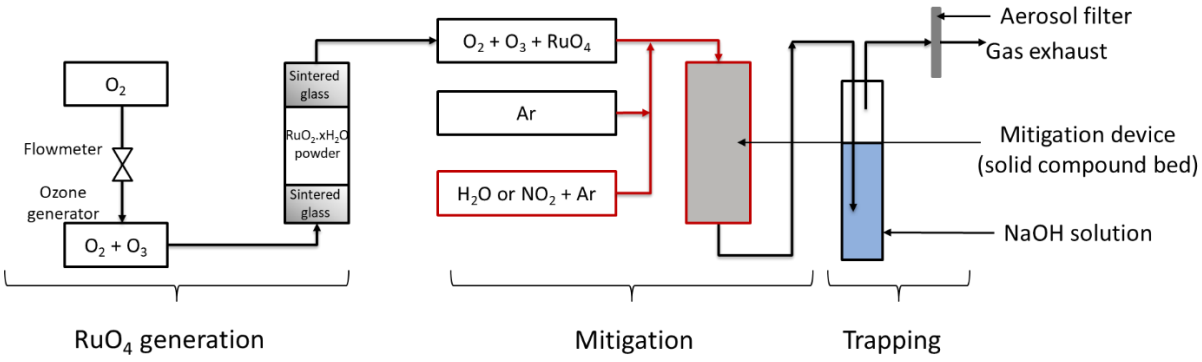

Figure 1: Experimental device: SAFARI test bench for Ru mitigation by solid compounds.

Gaseous ruthenium tetroxide is generated in a glass sintered column with a diameter of 2 cm, containing 400 mg of $RuO_2 \cdot xH_2O$ commercial powder. Oxidation of this powder is achieved using ozone from an ozone generator and dioxygen tank, leading to gaseous ruthenium tetroxide:

$$RuO_2(s) + 2/3\ O_3\ (g) \rightarrow RuO_4(g) \quad (1)$$

Dioxygen flow is set at 0.06 $NL.min^{-1}$ with a concentration of 45 $g.m^{-3}$ of ozone. The gaseous flow containing $RuO_4 + O_2 + O_3$ is then mixed with H_2O and/or NO_2 diluted in argon (instead of air to avoid N_2 oxidation by residual O_3) to obtain the target velocity of 10 $cm.s^{-1}$ through the material bed (representative of gas flow through FCVS in accidental condition [14]). The desired gaseous flow is then directed in the mitigation device containing the studied material in a sintered column of 1 cm diameter. This material device is heated at 50 or 90 °C depending on the conditions studied. For some additional tests in presence of nitrogen dioxide and water vapour, NO_2 concentration is set to 100 ppmV using a 1000 ppmV NO_2/air bottle. Besides, distinct concentrations of water vapour are generated at 50 and 90°C in order to achieve a targeted humidity of 30% RH.

On the third part of the experimental device, the generated gaseous flow is passed through an aqueous solution of sodium hydroxide NaOH (0.05 $mol.L^{-1}$) in order to trap all the incoming gaseous ruthenium tetroxide. In this alkaline medium, ruthenium tetroxide decomposes to ruthenate and perruthenate ions:

$$2\ RuO_4(g) + 2\ HO^-(aq) \rightarrow 2\ RuO_4^-(aq) + ½\ O_2(g) + H_2O(aq) \quad (2)$$

$$2\ RuO_4(g) + 4\ HO^-(aq) \rightarrow 2\ RuO_4^{2-}(aq) + O_2(g) + 2\ H_2O(aq) \quad (3)$$

Amounts of ruthenium trapped in this alkaline solution are determined by ICP-AES analyses. In order to determine the $RuO_4(g)$ generation rate (*i.e.* amount of ruthenium upstream the material bed), a by-pass line is added to the SAFARI bench, directly from RuO_4 generation column to a bubbler with sodium hydroxide solution (1 $mol.L^{-1}$).

Figure 2 presents a picture of SAFARI experiment.

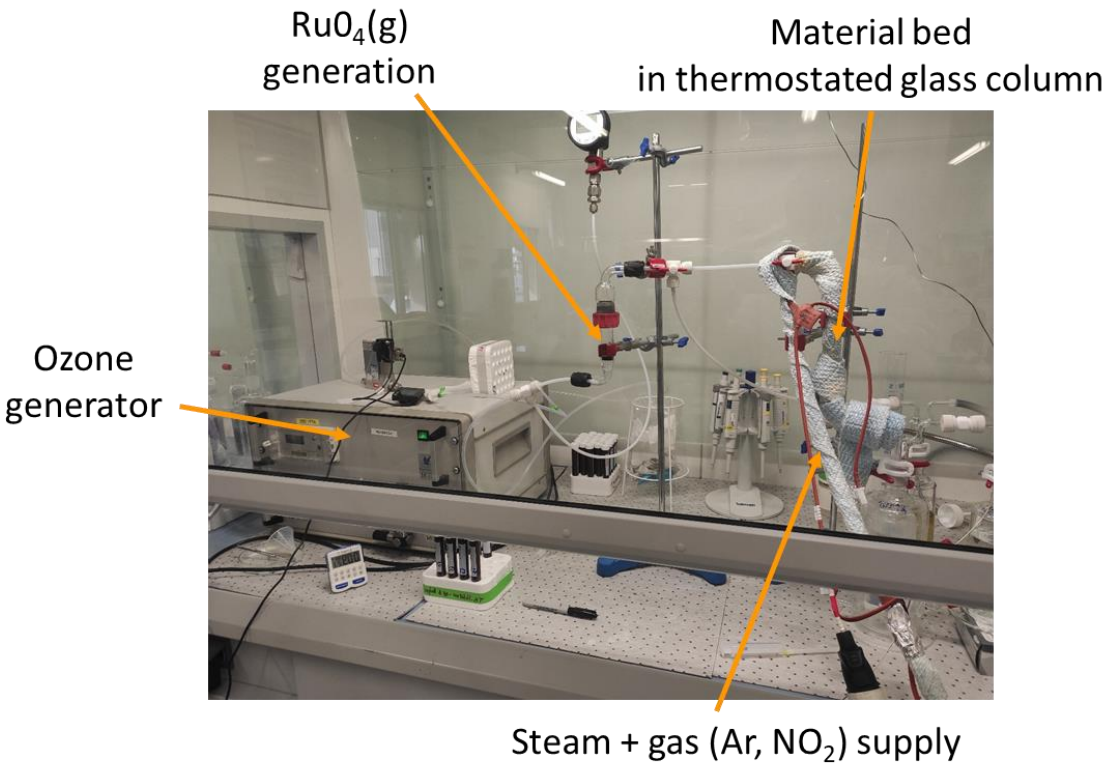

Figure 2: SAFARI experiment.

2.2. Decontamination factor calculation

The objective of SAFARI test bench is to evaluate the mitigation efficiency of the material used for the filtration (MOF, silica, cerium oxide). Hence, the decontamination factor (DF) has to be calculated (equation 4), *i.e.* the ratio of RuO_4 concentration upstream and downstream the material bed:

$$DF_{RuO4} = [RuO_4]_{upstream}/[RuO_4]_{downstream} \quad (4)$$

- Ru amounts generated in the upstream part are estimated thanks to the by-pass line mentioned above: before each experiment, ruthenium tetroxide is generated for one hour and trapped in an aqueous solution of sodium hydroxide (1M). Samplings are realized each 15 minutes over a period of one hour to estimate ruthenium tetroxide generation rate (expressed in μg_{RuO4}/min). At the end of the experiment, this process can be re-iterated to confirm the kinetics of ruthenium tetroxide generation for a given test. The RuO_4 generation rate can vary between tests performed on different days/weeks (range approximately from 450 to 1600 μg_{RuO4}/min), due to the sensitivity of ozone generator. This explains why it is calibrated for each test.
- The determination of Ru amounts downstream the tested material is carried out as follows: a sampling is realized every 30 minutes; it is then possible to calculate the ruthenium tetroxide mass that passed through the material bed.

Thus, knowing the cumulated ruthenium tetroxide quantity downstream the mitigation device after each sampling and the expected ruthenium tetroxide generation rate, it is possible to calculate the decontamination factor at any given time during the retention process following the equation 5:

$$DF = \frac{m(Ru_{cumulated})_{upstream}}{m(Ru_{cumulated})_{downstream}} \quad (5)$$

It is consistent with the previous equation (concentrations ratio) since the total flow rate remains constant during all the experiment.

In the following, the evolutions of DF values during a test will be used to assess if the breakthrough of the material bed has been achieved by gaseous RuO_4. Actually, the breakthrough is considered to be

reached when DF decreases continuously over the test (from high values in first samplings), to reach a value below 10^2 (equivalent of a retention efficiency Eff of 99 %, with Eff = 1 - 1/DF,). During an experiment, it corresponds to the emergence of a yellow/green colour in NaOH bubbler downstream the tested material, characteristic of ruthenate and perruthenate ions (equations 2 and 3).

2.3. Materials tested

Previous investigations on the interaction of gaseous RuO_4 with some materials composing the inner surfaces of containment buildings have shown that the black Ru-containing deposits mainly consist of a hydrated form of RuO_2 oxide (in +IV oxidation state) [33]. Hence, this shows that materials possessing a redox reducing activity could possibly act as efficient solid traps for RuO_4 because they will promote its reduction to RuO_2. Among the tested adsorbents which were found successful for iodine trapping, hybrid adsorbents such as MOFs or nanosilicas functionalized with amine groups are also suitable candidates for RuO_4 retention. Cerium oxide based-materials used in automotive catalysts were also targeted because of their well-known oxygen buffer capacity (OSC) associated with the easy switch between Ce +IV and +III oxidation states [34]. By contrast, as mentioned in the introduction, preliminary tests carried out with zeolites in silver or protonated forms did not show any appreciable activity for Ru reduction and were discarded for this study, as well as tests with activated charcoals [17].

2.3.1. Description of UiO-66-NH_2

The Zr-based UiO-66-NH_2 belongs to the porous MOF material family and has been chosen for this study because of its stability under severe conditions and its very good affinity for volatile fission products such as iodine [26] and ruthenium [28], its straightforward synthesis, but also its structural organization, that we suppose well adapted for the capture and the confinement of RuO_4. Indeed, UiO-66-NH_2 (Figure 3) is built up from the assembly of Zr-centered oxo/hydroxo hexanuclear clusters with aminoterephtalate ligands, giving rise to two types of cavities (octahedral or tetrahedral shape), which are accessible through windows slightly larger (5 Å) than the estimated diameter of RuO_4 (4.5 Å). Its synthesis has been carried out in our laboratory following the procedure described in reference [28]. In this study, we used UiO-66-NH_2 from a batch synthesized on a large scale, presenting a specific surface area (BET model) of 825 $m^2.g^{-1}$ and pore volume of 0.31 $cm^3.g^{-1}$ [25][28]. Based on ^1H NMR analysis, the formula of this solid is $Zr_6O_4(OH)_4(BDC\text{-}NH_2)_{4,55}(form)_{2.90}$ (BDC-NH2 = 2-aminoterephtalate; form = formate). The presence of formate groups in the structure indicates a partial substitution of aminoterephtalate linkers by formate species, as usually observed in this type of structure [35].

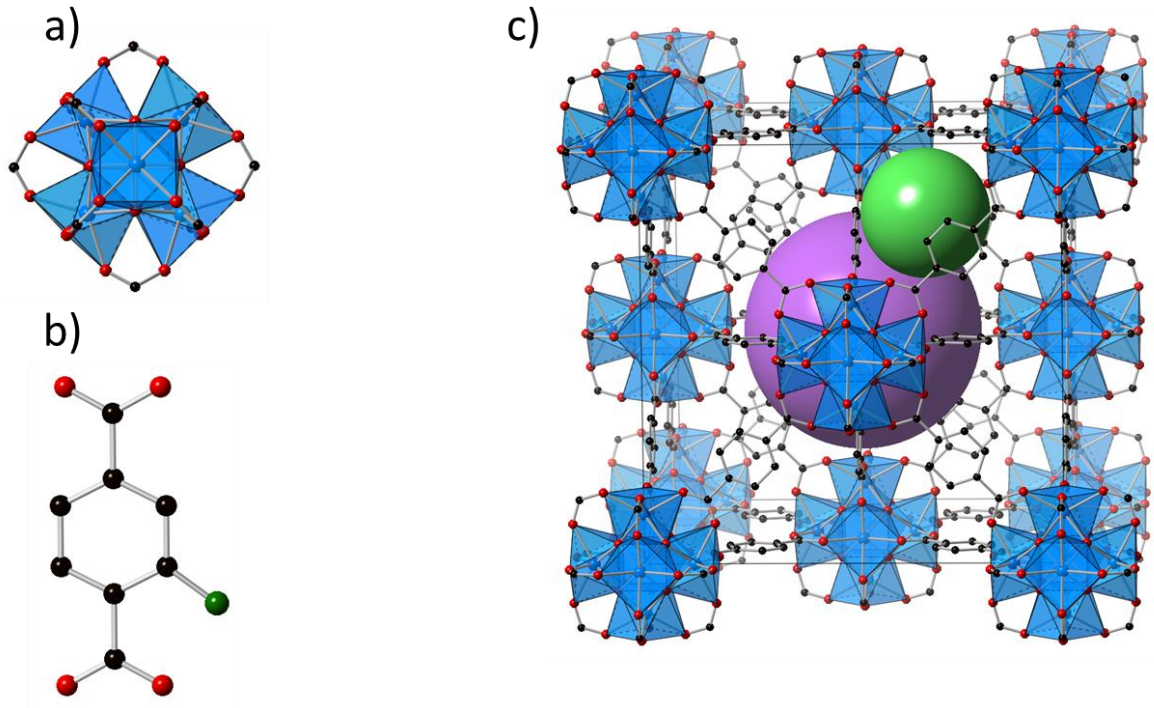

Figure 3: Schematic structural illustration of UiO-66-NH_2. a) $[Zr_6O_4(OH)_4]^{12+}$ cluster as secondary building unit (SBU), b) 2-aminoterephthalate carboxylate (BDC-NH_2) as an organic linker, and c) the face-centred-cubic (fcc) crystal structure of UiO-66-NH_2. Purple sphere: octahedral cavity; green sphere: tetrahedral cavity; NH_2 groups are omitted for clarity, due to disordered configuration.

2.3.2. Other compounds

The two following solid compounds have been tested on SAFARI test bench:

- PEI-Aerosil, which corresponds to a modified commercial silica material (Aerosil 380, from Evonik) with an amine-containing polymer: polyethylenimine (PEI). The PEI dissolved in methanol solvent was incorporated by impregnation of the silica powder (10 g) to reach a PEI content of 23%wt. Figure 4 represents PEI-Aerosil.

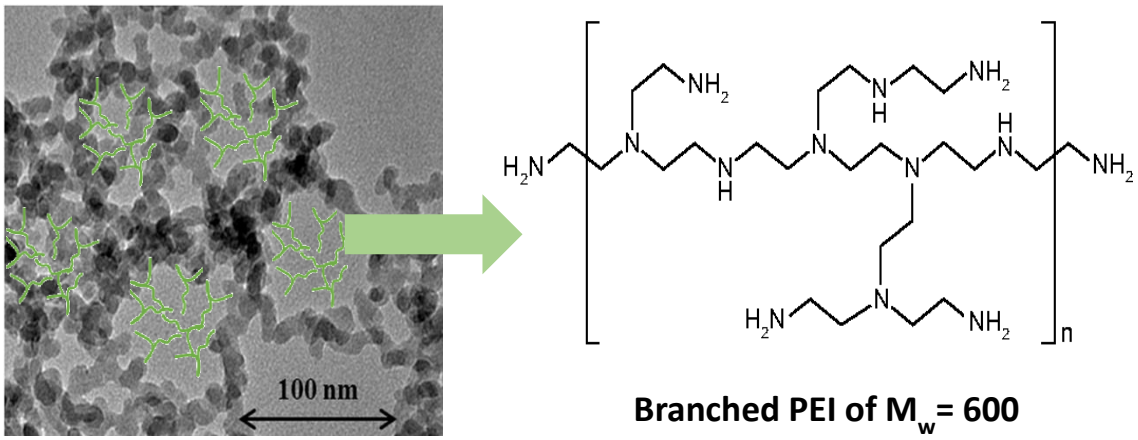

Figure 4: Structure of PEI-modified Aerosil silica.

- Cerium dioxide (CeO_2) powder has been purchased from Sigma-Aldrich (reference 544841, batch MKCQ5062, average particle size BET: 17 nm) and was used directly. Figure 5 represents the fluorite structure of CeO_2.

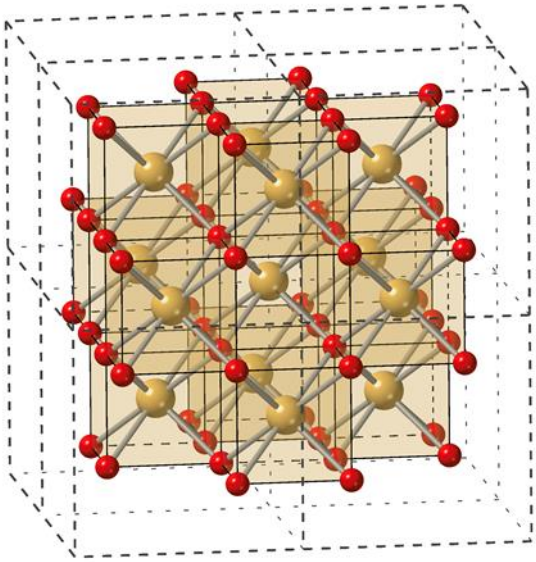

Figure 5: Structure of cerium dioxide $Ce0_2$. Yellow spheres: cerium; red spheres: oxygen.

2.4. Tests matrix

To complete the results obtained in smooth (model) conditions on the promising material UiO-66-NH_2 for RuO_4 trapping [28] and explore the other compounds presented above, the tests series detailed in Table 1 has been proposed. For MOF UiO-66-NH_2, the different parameters are studied as follows (MOF-X stands for UiO-66-NH_2 with a test letter X):

- Test MOF-A: reference experiment without nitrogen dioxide nor steam and with a material bed thickness of 1 cm.
- Test MOF-B: influence of material bed thickness (2 cm).
- Tests MOF-C and MOF-D: steam influence (H_2O) for two temperatures. Indeed, important quantities of steam can be present in severe accident scenario on PWR, as well as for loss of cooling system scenario in high level liquid waste PF tanks.
- Tests MOF-E and MOF-F: influence of nitrogen dioxide in gas mixture.
- Tests MOF-G and MOF-H: combinations of steam and nitrogen dioxide influence in gas mixture.
- Tests SIL-1, SIL-2, CER-1 and CER-2: same conditions as tests MOF-A and MOF-G, respectively with PEI Aerosil and cerium dioxide as material.

For each test, the material sample is first dried out in oven (120 °C, 30 min) and introduced in the sintered column. Then the tested material in mitigation device column is heated at 50 °C (reference) or 90 °C. These two heating steps before RuO_4, steam or NO_2 injection (depending on the test, cf. Table 1) contribute to ensure that solids contain no residual water before exposure to the expected gas mixture.

In the case of UiO-66-NH_2, due to the relative low temperature of activation (<150°C), this MOF is considered in a hydroxylated state [36]. The reaction between $RuO_2 \cdot xH_2O$ and ozone is carried out at room temperature. The choice of 90 °C for several tests allows to avoid the thermal degradation of RuO_4 (for $T \geq 108$ °C) [14], while approaching the temperature reached in accidental situation. As mentioned above, velocity of gas mixture is fixed at 10 $cm.s^{-1}$, so the different gas flow rates (Ar, steam, NO_2) are adapted to this target.

Table 1: Test matrix.

Test	Material	Studied parameter	Material bed thickness (cm)	T (°C)	Humidity (% RH)
MOF-A	UiO-66-NH_2	Reference	1	50	0
MOF-B		Bed thickness	2	50	0
MOF-C		H_2O influence	1	50	30
MOF-D			1	90	30
MOF-E		NO_2 influence (1^{st} phase with NO_2 only in MOF-5bis	1	50	0
MOF-Ebis			1	50	0
MOF-F			1	90	0
MOF-G		H_2O + NO_2 influences	1	50	30
MOF-H			1	90	30
SIL-1	Modified silica PEI aerosil	Reference	1	50	0
SIL-2		H_2O + NO_2 influences	1	50	30
CER-1	Cerium dioxide powder	Reference	1	50	0
CER-2		H_2O + NO_2 influences	1	50	30

3. RESULTS

3.1. Performances of UiO-66-NH_2 for RuO_4 retention

3.1.1. Decontamination factors measurements

On Figure 6 are displayed the evolutions of decontamination factors as a function of time, for tests MOF-A to MOF-G, with UiO-66-NH_2.

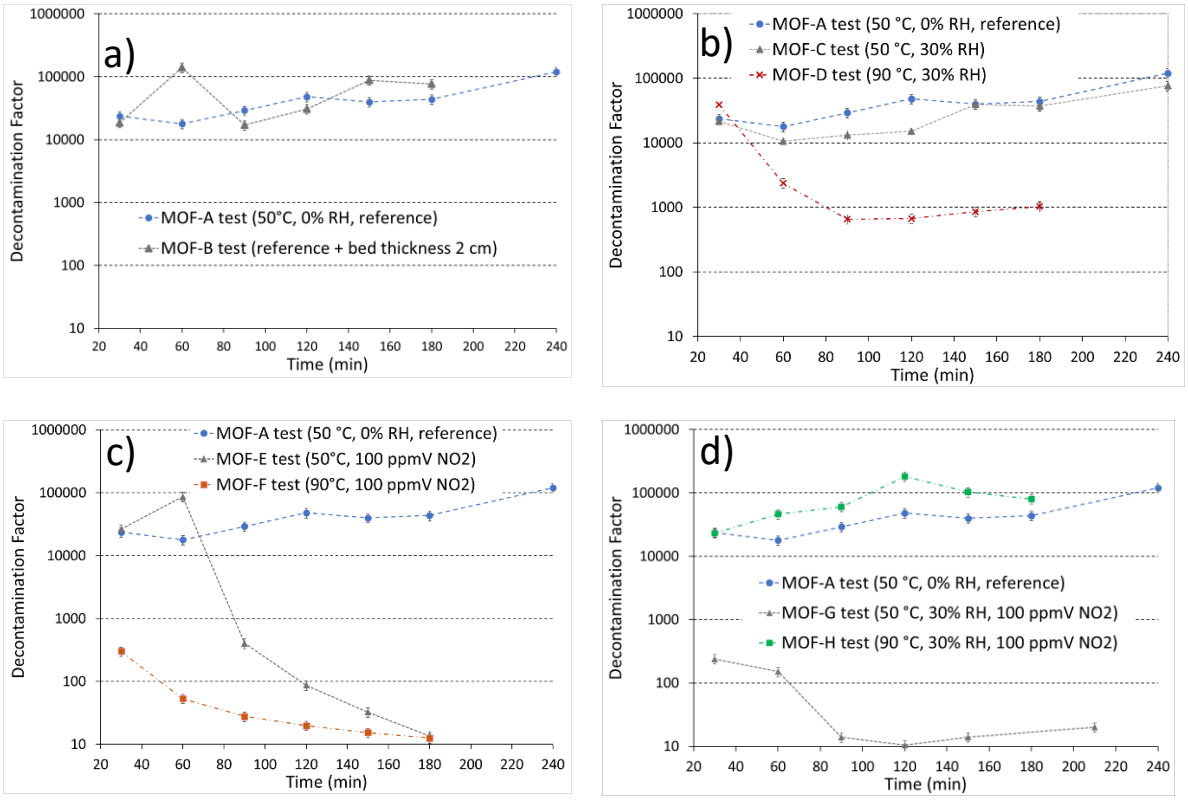

Figure 6: Decontamination factors for RuO_4 in UiO-66-NH_2 as a function of time. a) Reference test and influence of bed thickness; b) Influence of H_2O vapour (30% RH); c) Influence of NO_2 100 ppmV; d) Combined influence of NO_2 (100 ppmV) and H_2O vapour (30% RH).

3.1.2. X-ray diffraction analysis

Figure 7 presents X-ray diffraction patterns of spent materials resulting from tests MOF-A to MOF-H, compared to the X-ray diffractogram of the unreacted MOF UiO-66-NH_2. Powder X-ray diffraction diagrams have been collected at ambient temperature using a diffractometer Bruker D8 Advance A25. The measurement conditions are: $5° \leq 2\theta \leq 50°$; step: 0.02°; acquisition: 0.5 s/step.

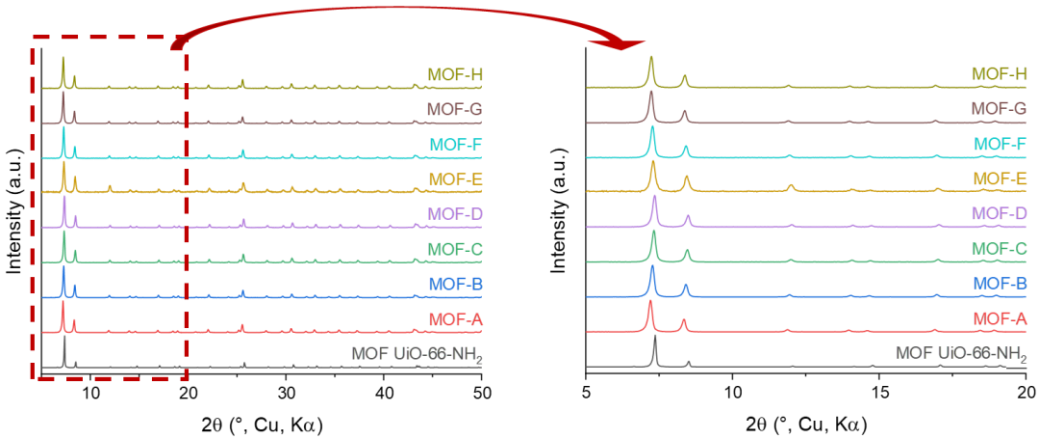

Figure 7: Powder X-ray diffraction patterns of MOF UiO-66-NH_2 before RuO_4 retention and after tests MOF-A to MOF-H (radiation: copper wavelength). $5° \leq 2\theta \leq 50°$; step: 0.02°; acquisition: 0.5 s/step. Right: focus on small angles.

3.2. Alternative compounds: PEI-modified organo-silica and cerium dioxide

The two other materials studied for ruthenium tetroxide mitigation are PEI-modified Aerosil silica and a high specific surface area cerium dioxide powder, as described in section 2.3.2. For each compound, two experiments have been performed at 50 °C with 1 cm of material bed thickness and a velocity of 10 $cm.s^{-1}$ through the material (cf. test matrix in Table 1, section 2.4):

- reference test (dry gas at 50 °C, SIL-1 and CER-1 tests), for comparison with MOF-A test,
- influence of steam (30 % RH) and NO_2 (100 ppmV in gas mixture), SIL-2 and CER-2 tests, for comparison with MOF-G test.

Figure 8 presents the results obtained in tests SIL-1 and SIL-2.

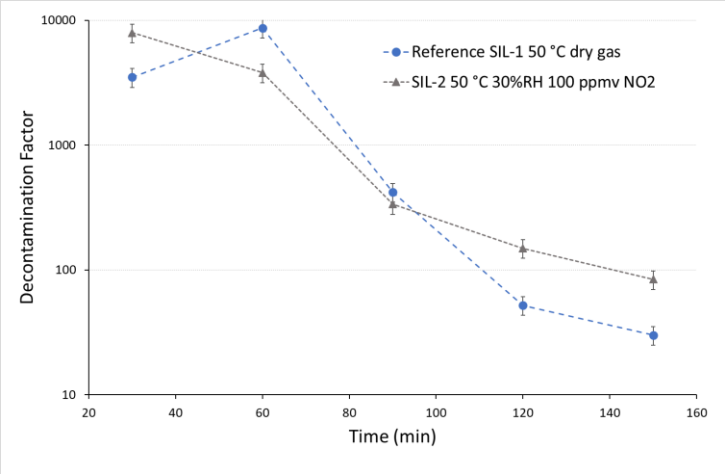

Figure 8: Decontamination factor as a function of time for RuO_4 in Silica PEI-Aerosil experiments.

For cerium dioxide CeO_2, in reference test CER-1 at 50 °C, decontamination factor remains close to 1 from the beginning of the test until the final measurement. The result is almost the same in presence of steam and NO_2 (test CER-2).

3.3. RuO_4 generation rates and material trapping capacities

For each test performed, Table 2 summarizes RuO_4 generation rates, evaluated as described in section 2.2, and material trapping capacities.

Table 2: Summary of RuO_4 generations and material trapping capacities for tests involving UiO-66-NH_2 and PEI-modified Aerosil silica

Test	RuO_4 generation rate (μg_{RuO4}/min ±12%)	Ru trapping capacity ($mg_{Ru}/g_{compound}$ ±12%)	Observations*
MOF-A	730	366	Quantity after 180 min No breakthrough
MOF-B	760	192	Quantity after 180 min No breakthrough (more material: 2 cm bed thickness)
MOF-C	480	245	Quantity after 180 min No breakthrough
MOF-D	1350	248	Quantity after 60 min Decrease of efficiency between 30 and 60 min but remains around 600 <DF < 1000
MOF-E	1230	309	Quantity after 60 min Breakthrough between 60 and 90 min
MOF-F	1466	120	Quantity after 30 min Breakthrough between 30 and 60 min
MOF-G	1200	210	Quantity after 60 min Breakthrough between 60 and 90 min
MOF-H	1160	Black deposit on glass column upstream material bed	-
SIL-1	1070	152	Quantity after 60 min Breakthrough between 60 and 120 min (continuous decrease even if DF > 100 after 90 min)
SIL-2	1656	237	Quantity after 60 min Breakthrough between 60 and 150 min (continuous decrease even if DF > 100 after 90 min)
CER-1	988	-	Immediate breakthrough
CER-2	638	-	Immediate breakthrough

*Breakthrough mentioned are confirmed by yellow/green colouring in NaOH bubbler at the indicated time

4. DISCUSSION

4.1. UiO-66-NH_2

4.1.1. Reference test and bed thickness

On Figure 6-a, values of measured decontamination factors for reference test MOF-A (blue), are ranging between 10^4 and 10^5 according to time. No breakthrough of ruthenium tetroxide over UiO-66-NH_2 material was observed after 240 min of test. Inside the adsorbent bed, Ru is very probably in hydrated RuO_2 form in view of its typical black colour. This retention ability and observations are consistent with previous results [28]. DF-value seems to slightly increase as a function of time maybe due to auto-catalytic effect induced by RuO_2 deposits. At the end of MOF-A test (4 h), the amount of Ru trapped in UiO-66-NH_2 was calculated (on the basis of RuO_4 generation rate mentioned in Table 2) to be around 488 mg_{Ru}/g_{MOF} (±12%,). Here, it is worth noting that the measured adsorption capacity could have been higher if the test duration was extended to a longer period of time (no breakthrough so no saturation of UiO-66-NH_2 by Ru). In Table 2, a reference value of around 366 mg_{Ru}/g_{MOF} (±12%) after 180 min of test was used to compare the results with other tests performed using other operating conditions.

In MOF-B experiment, 2 cm of adsorbent material (instead of 1 cm) were used in the sintered column, other parameters being the same as the reference test. Within experimental errors, the temporal evolution of decontamination factors (Figure 6-a), grey), remained roughly similar as test MOF-A (blue) with DF values in the range 10^5-10^4. At the end of the test (180 min), the quantity of Ru trapped in UiO-66-NH_2 was determined to be around 192 mg_{Ru}/g_{MOF} (±12%), *i.e.* approximately the half of the reference. This result was expected since no breakthrough happened with 1 cm of material in the same operating conditions. Thus, only 1 cm of material was used in the next experiments.

4.1.2. Influence of H_2O vapour (relative humidity)

Steam being present in case of nuclear accident, two experiments were carried out in presence of water vapour, at 50 and 90 °C (Figure 6-b, in dark grey and red, respectively). Both experiments were conducted with a constant relative humidity (RH) of 30%.

- At 50 °C (test MOF-C), no breakthrough was observed even after 4h of test. DF measurements, between 10^4 and 10^5, witness of an efficient trapping of ruthenium tetroxide by the UiO-66-NH_2 material (DF evolution similar to reference test MOF-A) even in presence of humidity. The quantities of Ru trapped in the MOF were determined to be around 245 mg_{Ru}/g_{MOF} (±12%) after 180 min and 327 mg_{Ru}/g_{MOF} (±12%) after 240 min. These values are slightly lowered than those of reference test due to some differences existing in the RuO_4 generation rate from one test to another, as stated in part 2.2.
- At 90 °C (test MOF-D), decontamination factors were higher than 10^5 after 30 minutes and decreased to around 10^3 after 1 hour while remaining rather stable after 90 min (til the end of experiment at t = 180 min). The slight decrease of DF values between 30 and 60 minutes has not to be attributed to the breakthrough of the adsorbent bed but rather to the role of water with saturation of some pores. The lower DF values after 1 hour in test D (90 °C) compared to test C (50 °C) could be explained by some differences pertaining to the amounts of water present in UiO-66-NH_2 material. Indeed, for 30% RH, the steam flowrate is 3.50 $g.h^{-1}$ at 90 °C *vs.* 0.69 $g.h^{-1}$ at 50 °C.

  Overall, the effect of humidity at 50 and 90°C was not found to be detrimental for RuO_4 retention. The quantities of Ru trapped in UiO-66-NH_2 were around 124 mg_{Ru}/g_{MOF} (±12%) after 30 min, 248 mg_{Ru}/g_{MOF} (±12%) after 60 min and 744 mg_{Ru}/g_{MOF} (±12%) after 180 min.

4.1.3. Influence of NO_2

Another studied parameter for the UiO-66-NH_2 material is the impact of nitrogen dioxide (NO_2) on ruthenium tetroxide mitigation by UiO-66-NH_2 material. Indeed, in the studied scenario in reprocessing plants, nitrogen oxides can be released in important quantities from boiling nitric solution to the atmosphere and can poison the adsorption sites of UiO-66-NH_2, to the detriment of ruthenium tetroxide simultaneously released during its transport.

In the literature, Peterson et al. [37] have shown that UiO-66-NH_2 presents high performances for NO_2 removal up to 1.4 g of NO_2/g MOF in air/steam atmosphere at 150 °C, capacity enhanced in presence of steam. The mechanism involves some redox reactions impacting the ligand structure of the MOF with the formation of nitrates and diazonium species and the possible release of N_2. In another study performed under ambient conditions, the bond between the organic linker and metallic oxide center is broken, leading to the formation of nitrate and nitrite species while organic ligands also contribute to the NO_2 reactive adsorption via nitration reaction [38]. Besides, it can also be expected that NO_2 could have a negative influence on RuO_2 deposits because of its highly oxidizing character, leading possibly to their re-volatilization as RuO_4 gas. However, this process should be limited due to the small concentrations used in our experiments (100 ppmV). Overall, it can be expected that trapping of RuO_4 decreases in presence of NO_2. Tests described hereafter allow to quantify this effect.

Experiments in dry gas

The experiments were carried out with 100 ppmV of nitrogen dioxide, at 50 and 90 °C (Figure 6-c). Ruthenium generation is around 1230 μg_{RuO4}/min (±12%) for test MOF-E (50 °C) and 1466 μg_{RuO4}/min for test MOF-F (90 °C). These quantities correspond to a molar ratio NO_2/RuO_4 of 0.21 for test MOF-E and 0.17 for test MOF-F. It highlights that NO_2 is not in excess in gas mixture (this would remain true even if RuO_4 generation rate was set to the minimum obtained during the whole set of experiments reported in Table 2, *i.e.* a molar ratio of 0.54 for a generation rate of 480 μg_{RuO4}/min).

- At 50 °C (test MOF-E), no breakthrough of the material was observed in the first hour of test ($10^4 < DF < 10^5$) but only after 90 min of experiment, since the decontamination factor decreased below 10^3 and then reached a value around 10 at the end of the experiment (180 min). The quantity of Ru trapped within UiO-66-NH_2 corresponded to 309 mg_{Ru}/g_{MOF} (±12%) after 60 min.
- At 90 °C (test MOF-F), the decontamination factor measured after 30 min is around 300, and below 10^2 after 60 min. It decreases to ~10 at the end of the experiment (180 min), similarly to what was observed at 50 °C. Thus, breakthrough seems to occur more rapidly at 90 than at 50°C. The quantity of Ru trapped in UiO-66-NH_2 is around 120 mg_{Ru}/g_{MOF} (±12%) after 30 min.
- Additional test MOF-Ebis has been conducted at 50 °C in two phases:
    - Step 1: exposition of MOF UiO-66-NH_2 to NO_2 without RuO_4 (1 hour),
    - Step 2: RuO_4 injection without NO_2.

  Breakthrough occurred quickly as in test MOF-F, with DF = 170 after 30 min (step 2) and DF below 40 after 1 hour. It confirms the inhibiting effect of NO_2 on RuO_4 trapping by UiO-66-NH_2. Indeed, the pre-exposure to NO_2 seems to degrade irreversibly adsorption sites due to its very oxidizing properties.

Despite NO_2 is not in molar excess with respect to RuO_4, nitrogen dioxide degrades the ability of UiO-66-NH_2 for RuO_4 trapping, more precisely the availability of the amine group to reduce RuO_4(g) in hydrated RuO_2(s) (this latter being observed inside the UiO-66-NH_2 after tests with trapping). The increase of temperature from 50 to 90 °C seems to enhance the poisoning effect of NO_2.

Combined influence of NO_2 + H_2O

The last tests with UiO-66-NH_2 aim at highlighting the combined influence of both nitrogen dioxide and steam on RuO_4 mitigation. (Figure 6-d). At 50 °C (30% RH and 100 ppmV NO_2), breakthrough seems

to occur just after the first hour of test: decontamination factor is in the range 100 < DF < 250 until 60 min, which is less than in the beginning of test MOF-E at 50 °C (0% RH and 100 ppmV NO_2) after 60 min. Thus, at 50°C, the impact of both NO_2 and steam (30% HR) on RuO_4 trapping capacities by UiO-66-NH_2 (MOF-G) is almost similar to that of NO_2 without water vapour (MOF-E).

At 90 °C and 30% RH (test MOF-H), the decontamination factors were very high, between 1000 and 100 000 (higher than in reference test MOF-A). However, in this configuration, ruthenium tetroxide was observed to decompose rapidly into ruthenium dioxide since a black deposit appeared on the sintered column (Figure 9). For this reason, no ruthenium tetroxide went through the filtration material as it degraded before the MOF in presence of steam and NO_2. This behavior is reminiscent of the thermal decomposition of RuO_4, notably observed in Nerisson et al. [14] for higher temperatures (> ~108 °C). This could be explained by a localized overheating phenomenon at the column head, which did not occur during the other tests at 90 °C.

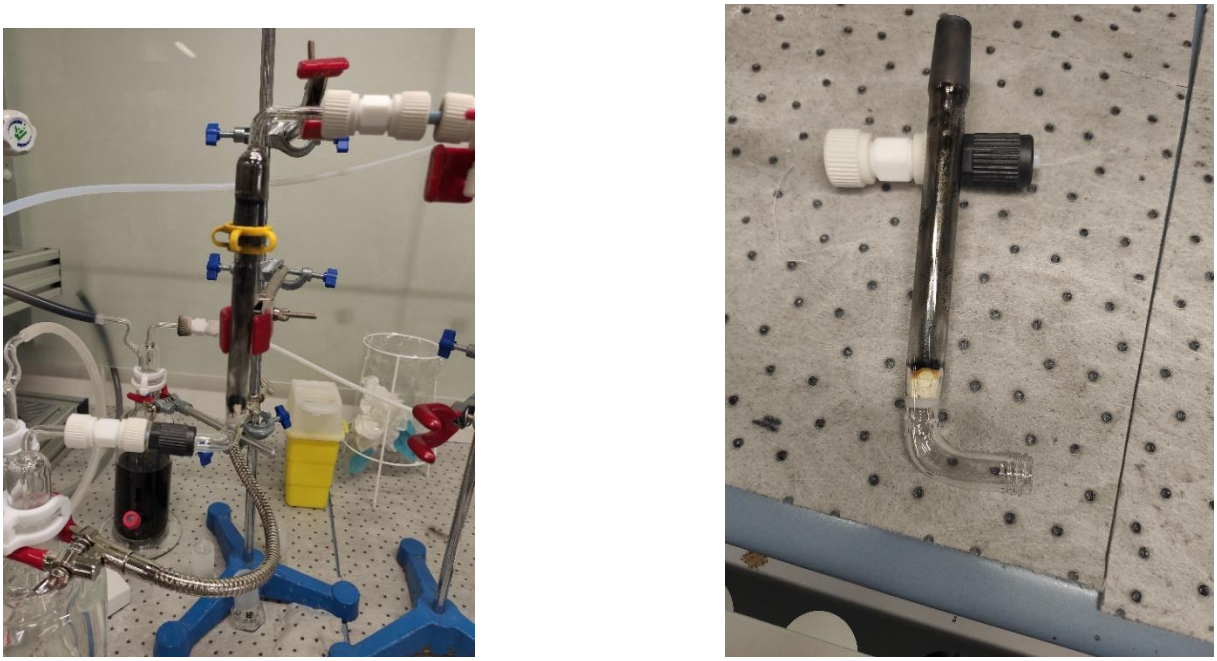

Figure 9: Sintered column containing UiO-66-NH_2 after MOF-H test.

4.1.4. X-ray diffraction

As shown on Figure 7, X-ray diffraction did not reveal any crystalized ruthenium oxide that would correspond to nanoparticles of metallic ruthenium trapped either inside or outside the UiO-66-NH_2, which is consistent with the study by Leloire et al. [25][28]. Hence, ruthenium dioxide must be present as an amorphous form, as described by McKeown et al. [39]. X-ray diffraction patterns of spent materials resulting from tests MOF-A to MOF-H were compared to the X-ray diffractogram of the unreacted MOF UiO-66-NH_2. For each test, an attenuation of Bragg main peaks associated with UiO-66-NH_2 is observed, which is linked to the incorporation of amorphous RuO_2 within the framework. In fact, the incorporation of amorphous RuO_2 does not lead to a partial degradation of the MOFs. Indeed, a proof was given in our previous work about UiO-66-NH_2 [25][28]. The crystallinity of UiO-66-NH_2 framework was still preserved, but the occurrence of large amount of amorphous RuO_2 within the pores led to a slight loss of intensity of the major diffraction peaks. Although a deep after-test characterization

was not performed for the other tested materials (cf. sections 3.2 and 4.2), the presence of a black amorphous deposit of RuO_2 was observed for all kinds of adsorbents.

4.2. Alternative compounds

4.2.1. PEI-modified organo-silica

In reference test SIL-1 at 50 °C, no breakthrough is observed until 1 hour. This corresponds to decontamination factors between 10^3 and 10^4 (Figure 8). Then, the decontamination factor decreases, to reach DF = 30 after 150 min implying that breakthrough of silica bed occurs between 60 and 120 min of experiment (continuous decrease even if DF > 100 after 90 min). In test SIL-2, almost the same DF evolution is observed (Figure 8), so there is no influence linked to the presence of steam and nitrogen dioxide.

4.2.2. Cerium dioxide

With $Ce0_2$, breakthrough seems to occur immediately at the beginning of the test, attesting that the used commercial cerium dioxide has no capacity for RuO_4 trapping at 50 °C. It is worth noting that this result somewhat contradicts some preliminary tests performed on other kinds of Ce-based materials, which showed a much better behaviour [17]. In the present study, a commercial CeO_2 sample was used instead because of its availability in large amounts and its more adapted shaping. However, it seems that it has not the required redox properties to promote the trapping of RuO_4 to hydrated RuO_2 deposits. Such properties can be obtained by using ceria nanoparticles of small size or doped with foreign elements in order to enhance the fraction of Ce^{3+} sites, which are needed for RuO_4 reduction. Indeed, it was shown that the presence of reduced cerium sites and oxygen vacancies are key for a number of applications involving these materials. An alternative would be to test different samples belonging to this class of materials in the future, in order to better understand the reactivity of Ce-based oxides.

4.3. Comparison of materials - Ru trapping capacities

This section focuses on MOF UiO-66-NH_2 and silica PEI-Aerosil (no trapping of RuO_4 with cerium dioxide, cf. 4.2.2).To allow a better comparison between these two materials in similar conditions (T, RH, NO_2 concentration), the time scale of a given test can be corrected by the ratio:

$$t_{corrected} = t_{reference}.{(RuO_4\ generation\ rate)_{test}}\Big/{(RuO_4\ generation\ rate)_{reference}} \quad (6)$$

According to results discussed in sections 4.1 and 4.2.1:

- in reference conditions (50 °C, dry gas), silica PEI-Aerosil is less efficient than UiO-66-NH_2 for RuO_4 trapping, since no breakthrough was observed with UiO-66-NH_2 for the same bed thickness (tests MOF-A and SIL-1). However, minimum breakthrough time for SIL-1 can be corrected to 87 min instead of 60 min, according to equation (6) with MOF-A as reference generation rate.
- in presence of steam and NO_2 at 50 °C, Figure 10 compares DF obtained for MOF-G and SIL-2 tests, using this time a corrected time scale for SIL-2, using equation (6) with MOF-G as reference generation rate. Silica appears more efficient than MOF, DF remaining above 100 after nearly 180 min of test for silica while it reaches a value close to 10 after 90 min for MOF.

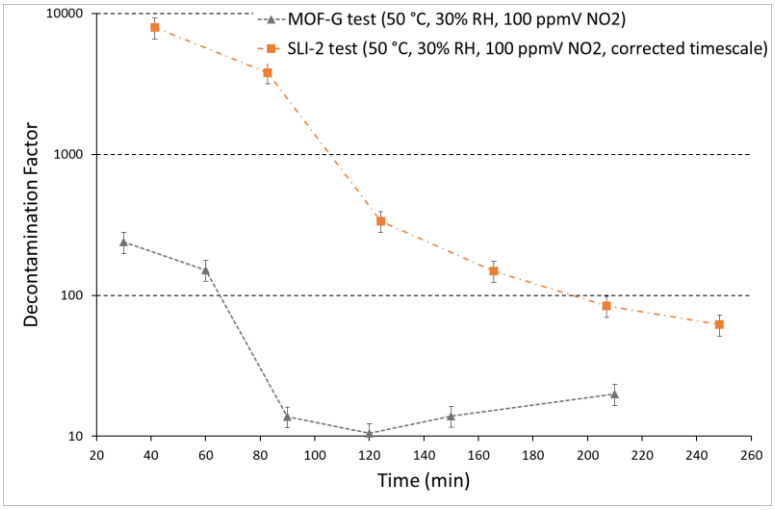

Figure 10: Decontamination factor as a function of time at 50 °C under mixture of H_2O (30% RH) and NO_2 (100 ppmV) for test MOF-G (grey triangles) and test SIL-2 (orange squares, corrected timescale according to equation (6) with MOF-G as reference generation rate)

More generally, breakthrough times can be influenced by RuO_4 generation rate. Thus, for tests where breakthrough occurred with UiO-66-NH_2 and silica PEI-aerosil, breakthrough times mentioned in Table 2 are corrected according to equation (6) with MOF-A as reference generation rate (730 μg_{RuO4}/min), and reported in Table 3. These are indicative values, the main result for each configuration tested being the occurrence (or not) of breakthrough and the order of magnitude of its timing. Besides, it should be remembered that:

- for tests without breakthrough (see Table 2), more RuO_4 could have been trapped with a longer test (for the same bed thickness),
- when breakthrough occurs, a fraction of incident RuO_4 may still be trapped after it. But in this latter case, the amount obtained can give the order of magnitude beyond which retention becomes not satisfactory.

Table 3: Corrected breakthrough time following equation (6) with MOF-A as reference test for RuO_4 generation, for tests where breakthrough occured involving UiO-66-NH_2 and PEI-modified Aerosil silica

Test	Corrected breakthrough time following equation (6) with MOF-A as reference test for RuO_4 generation
MOF-E	Breakthrough between 151 and 202 min
MOF-F	Breakthrough between 60 and 120 min
MOF-G	Breakthrough between 98 and 147 min
SIL-1	Breakthrough between 87 and 175min
SIL-2	Breakthrough between 136 and 340 min

As mentioned before, the black deposit is very probably in a hydrated amorphous black solid RuO_2 form, as described by Leloire et al. [25], [28]. Figure 11 shows the difference between two spent UiO-66-NH_2 beds collected after (right) or without breakthrough (left), respectively MOF-E and MOF-A. As

discussed above in section 4.1.3, NO_2 may partially inhibit RuO_4 reduction inside UiO-66-NH_2. Indeed, black deposit is visible all along the MOF bed in test MOF-E, while the top layer of the UiO-66-NH_2 bed is sufficient to trap all incoming RuO_4(g) in test MOF-A.

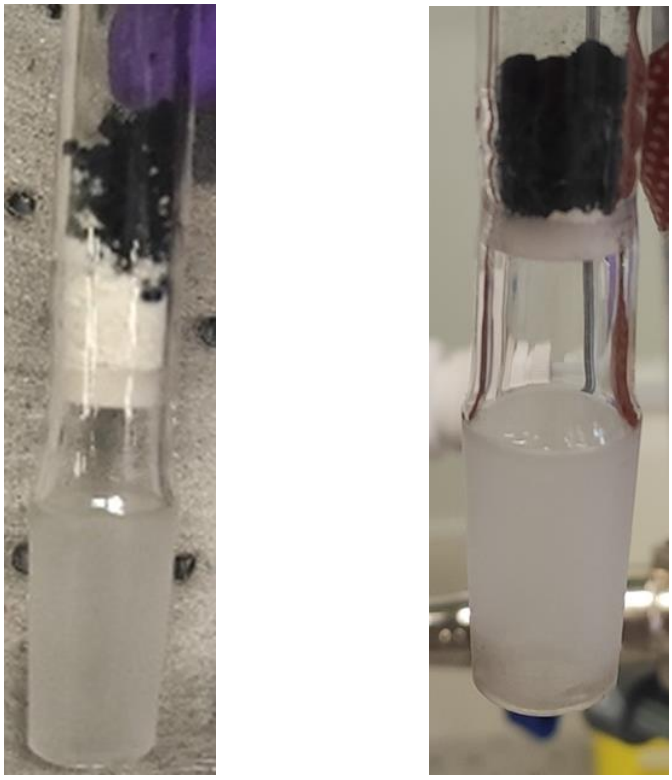

Figure 11: Evolution of the UiO-66-NH_2 powdered samples at the end of tests MOF-A (left, no breakthrough) and MOF-E (right, breakthrough reached)

5. CONCLUSIONS

Experiments of gaseous RuO_4 trapping in solid materials have been conducted on a dedicated test bench, with experimental operating parameters approaching conditions occurring in different nuclear accident scenarios, covering fuel cycle and nuclear power plants.

RuO_4 trapping efficiency is confirmed for UiO-66-NH_2 at 50 °C in dry gas, with DF > 10^4. This order of magnitude of DF is also observed with higher bed thickness and with steam at 50 °C. In presence of steam at 90 °C, DF decreases but remains high (DF > 10^3 after 60 min and DF > 600 at the end of the test). In presence of NO_2 in the feed gas, DF decreases significantly after approximately one hour of test, both at 50 and 90 °C due to alteration of amine groups. Indeed, breakthrough of 1 cm UiO-66-NH_2 bed by RuO_4 occurs between 60 and 90 min after starting the test. Efficiency remains acceptable before this breakthrough (DF > 100) and reaches a value in the range 10 < DF < 100 at the end of the tests. Nitrogen dioxide is confirmed to be very reactive with respect to amine groups present in MOF, in line with its oxidizing properties.

In dry conditions, PEI-modified Aerosil silica is less efficient than UiO-66-NH_2 for RuO_4 trapping but its capacity is preserved in presence of steam and NO_2, while its efficiency is better than UiO-66-NH_2 in these latter conditions.

The used commercial cerium dioxide powder (CeO_2) is not efficient for RuO_4 trapping whatever the conditions, despite encouraging previous results obtained with this class of materials. This could highlight a strong sensitivity to the characteristics of these materials, notably the Ce^{3+}/Ce^{4+} ratio, for RuO_4 trapping.

ACKNOWLEDGMENTS

This work was performed in the French Institut de Radioprotection et de Sûreté Nucléaire (IRSN), with the financial support of ORANO Recyclage. The authors would like to thank Laurence Burylo and Philippe Devaux for their assistances with the preliminary synthesis and XRD powder patterns measurements (UCCS). The "Fonds Européen de Développement Régional (FEDER)", "CNRS", "Région Hauts de France" and "Ministère de l'Education Nationale de l'Enseignement Supérieur et de la Recherche" are acknowledged for the funding of X-ray diffractometers from the Chevreul Institute platform.

REFERENCES

[1] Masson O et al. (2019) Airborne concentrations and chemical considerations of radioactive ruthenium from an undeclared major nuclear release in 2017. Proc Natl Acad Sci 116(34):16750–16759. https://doi.org/10.1073/pnas.1907571116

[2] Giordano P, Auvinen A, Brillant G, Colombani J, Davidovich N, Dickson R, Haste T, Kärkelä T, Lamy JS, Mun C et al. (2010) Recent Advances in Understanding Ruthenium Behaviour Under Air-Ingress Conditions During a PWR SevereAccident. Prog Nucl Energy 52:109−119. https://doi.org/10.1016/j.pnucene.2009.09.011

[3] Pontillon Y, Ducros G (2010) Behaviour of Fission Products Under Severe PWR Accident Conditions. the VERCORS Experimental Programme−Part 3: Release of Low-Volatile Fission Products and Actinides. Nucl Eng Des 240:1867−1881. https://doi.org/10.1016/j.nucengdes.2009.06.024

[4] Kärkelä T, Vér N, Haste T, et al (2014) Transport of ruthenium in primary circuit conditions during a severe NPP accident. Ann Nucl Energy 74:173–183. https://doi.org/10.1016/j.anucene.2014.07.010

[5] Miradji F, Virot F, Souvi S, Cantrel L, Louis F, Vallet V (2016) Thermochemistry of ruthenium oxyhydroxyde species and their impact on volatile speciations in severe nuclear accident conditions. J Phys Chem A 120(4):606–614. https://doi.org/10.1021/acs.jpca.5b11142

[6] Miradji F, Souvi S, Cantrel L, Louis F, Vallet V (2022) Reactivity of Ru oxides with air radiolysis products investigated by theoretical calculations. J Nucl Mater 558:153395. https://doi.org/10.1016/j.jnucmat.2021.153395

[7] Ohnet MN, Leroy O, Mamede AS (2018) Ruthenium behavior in the reactor cooling system in case of a PWR severe accident. J Radioanal Nucl Chem 316:161–177. https://doi.org/10.1007/s10967-018-5743-2

[8] Blasius E, Glatz JP, Neumann W (1981) Ruthenium nitrosyl complexes in radioactive waste solutions of reprocessing plants. I. Cationic ruthenium nitrosyl complexes. Radiochim Acta 29(2-3):159-166. https://doi.org/10.1524/ract.1981.29.23.159

[9] Blasius E, Luxenburger HJ, Neumann W (1984) Ruthenium nitrosyl complexes in radioactive waste solutions of reprocessing plants. II. Ruthenium nitrosyl complexes in high-level wastes. Radiochim Acta 36:149-153.

[10] Blasius E, Muller K (1984) Ruthenium nitrosyl complexes in radioactive waste solutions of reprocessing plants. III. Behaviour of ruthenium nitrosyl complexes during storage, concentration and calcination. Radiochim Acta 37(4):217-222. https://doi.org/10.1524/ract.1984.37.4.217

[11] Philippe M, Mercier JP, Gué JP (1990) Behavior of ruthenium in the case of shutdown of the cooling system of HLLW storage tanks. Proceedings of the 21st DOE/NRC Nuclear Air Cleaning Conference:831-843. https://inis.iaea.org/search/search.aspx?orig_q=RN:35070205

[12] Mercier JP, Gue JP, Bonneval F, Martineau D, Philippe M (1991) An example of R&D on safety assessment: study of a prolonged loss of cooling of HALW (beyond design accident), Institut de Protection et de Sûreté Nucléaire. Proceedings of OECD/NEA/CSNI Specialist meeting on safety and risk assessment in fuel cycle facilities, Tokyo, Japan. https://www.oecd-

nea.org/jcms/pl_15892/csni-specialist-meeting-on-safety-and-risk-assessment-in-fuel-cycle-facilities-1991-tokyo-japan-1991?details=true

[13] Jacquemain D, Guentay S, Basu S, Sonnenkalb M, Lebel L, Ball J, Allelein H, Liebana M, Eckardt B, Losch N. et al. (2014) OECD/NEA/CSNI/R(2014)7 status report on filtered containment venting. https://www.oecd-nea.org/jcms/pl_19514/oecd/nea/csni-status-report-on-filtered-containment-venting?details=true

[14] Nerisson P, Hu H, Paul JF, Cantrel L, Vesin C (2019) Filtration tests of gaseous ruthenium tetroxide by sand bed and metallic filters. J Radioanal Nucl Chem 321(2):591-598. https://doi.org/10.1007/s10967-019-06612-8

[15] Ishio T, Shibata Y, Kodama T, Kato T, Tsukada T, Serrano-Purroy D, Glatz JP (2015) Study on radioactive material transport behavior from boiling/drying out high level liquid waste. Proceedings of Global 2015, paper 5164:1069-1075

[16] Yoshida N, Ohno T, Amano Y, Abe H (2018) Migration behavior of gaseous ruthenium tetroxide under boiling and drying accident condition in reprocessing plant. J Nucl Sci Technol 55(6):599-604. https://doi.org/10.1080/00223131.2018.1428121

[17] Nerisson P, Barrachin M, Cantrel L, Philippe M (2019) Volatilization and trapping of ruthenium under a loss of cooling accident on high level liquid waste (HLLW) storage tanks in reprocessing plants. Proceedings of International Nuclear Fuel Cycle Conference Global 2019, Seattle. https://www.ans.org/pubs/proceedings/article-46990/

[18] De Almeida L, Nerisson P, Barrachin M, Cantrel L, Mun C, Ricciardi L, Philippe M (2019) R&D programme on volatilization and transport behaviour of ruthenium under a loss of cooling accident on high level liquid waste (HLLW) storage tanks in reprocessing plants and mitigation strategies. Proceedings of Nuclear Energy Agency International Workshop on Chemical Hazards in Fuel Cycle Facilities Nuclear Processing – App C. Nuclear Safety NEA/CSNI/R(2019)9/ADD1. https://www.oecd-nea.org/jcms/pl_19916/proceedings-of-international-workshop-on-chemical-hazards-in-fuel-cycle-facilities-nuclear-processing-appendix-c

[19] Ohnet MN, Boucault K, Nerisson P, Bagnol T, Cantrel L (2022) Experimental study of ruthenium volatilization from boiling nitric solution. J Radioanal Nucl Chem 331(7):2939-2953. https://doi.org/10.1007/s10967-022-08351-9

[20] Nerisson P, Barrachin M, Ohnet MN, Cantrel L (2022) Behaviour of ruthenium in nitric media (HLLW) in reprocessing plants: a review and some perspectives. J Radioanal Nucl Chem 331(9):3365-3389. https://doi.org/10.1007/s10967-022-08420-z

[21] Long JR, Yaghi OM (2009) The pervasive chemistry of metal–organic frameworks, Chem Soc Rev 38:1213-1214. https://doi.org/10.1039/B903811F

[22] Furukawa H, Cordova KE, O'Keeffe M, Yaghi OM (2013) The chemistry and applications of Metal-Organic Frameworks. Science 341(6149):1230444. https://www.science.org/doi/10.1126/science.1230444

[23] Xiao CL, Silver MA, Wang S (2017) Metal–organic frameworks for radionuclide sequestration from aqueous solution: a brief overview and outlook. Dalton Trans 46:16381-16386. https://doi.org/10.1039/C7DT03670A

[24] Falaise C, Volkringer C, Giovine R, Prelot B, Huve M, Loiseau T (2017) Capture of actinides (Th^{4+}, $[UO_2]^{2+}$) and surrogating lanthanide (Nd^{3+}) in porous metal–organic framework MIL-100(Al) from water: selectivity and imaging of embedded nanoparticles. Dalton Trans 46:12010-12014. https://doi.org/10.1039/C7DT02155K

[25] Leloire M (2021) Use of porous Metal-Organic Framework (MOF) for the adsorption of gas molecules (I_2, RuO_4) in case of a nuclear reactor accident. PhD thesis, Université de Lille, France. https://www.theses.fr/2021LILUR009

[26] Leloire M, Dhainaut J, Devaux P, Leroy O, Desjonqueres H, Poirier S, Nerisson P, Cantrel L, Royer S, Loiseau T, Volkringer C (2021) Stability and radioactive gaseous iodine-131 retention capacity of binderless UiO-66-NH_2 granules under severe nuclear accidental conditions. J Hazard Mater 416:125890. https://doi.org/10.1016/j.jhazmat.2021.125890

[27] Leloire M, Walshe C, Devaux P, Giovine R, Duval S, Bousquet T, Chibani S, Paul JF, Moissette A, Vezin H, Nerisson P, Cantrel L, Volkringer C, Loiseau T (2022) Capture of gaseous iodine in isoreticular zirconium-based UiO-n Metal-Organic Frameworks: influence of amino functionalization, DFT calculations, Raman and EPR spectroscopic investigation. Chem Eur J 28(14): e202104437. https://doi.org/10.1002/chem.202104437

[28] Leloire M, Nerisson P, Pourpoint F, Huvé M, Paul JF, Cantrel L, Loiseau T, Volkringer C (2022) Capture and Immobilization of Gaseous Ruthenium Tetroxide RuO_4 in the UiO-66-NH_2 Metal-Organic Framework. Dalton Trans 51:16170-16180. https://doi.org/10.1039/D2DT02371G

[29] Satyapal S, Filburn T, Trela J, Strange J (2001) Performance and Properties of a Solid Amine Sorbent for Carbon Dioxide Removal in Space Life Support Applications. Energ Fuel 15(2):250–255. https://doi.org/10.1021/ef0002391

[30] Hijazi A, Azambre B, Finqueneisel G, Vibert F, Blin JL (2019) High iodine adsorption by polyethyleneimine impregnated nanosilica sorbents. Micropor Mesopor Mat 288, 109586. https://doi.org/10.1016/j.micromeso.2019.109586

[31] Chebbi M, Azambre B, Monsanglant-Louvet C, Marcillaud B, Roynette A, Cantrel L (2021) Effects of water vapour and temperature on the retention of radiotoxic CH_3I by silver faujasite zeolites. J Hazard Mater 409:124947. https://doi.org/10.1016/j.jhazmat.2020.124947

[32] Lin H, Chebbi M, Monsanglant-Louvet C, Marcillaud B, Roynette A, Doizi D, Parent P, Laffon C, Grauby O, Ferry D (2022) KI and TEDA influences towards the retention of radiotoxic CH_3I by activated carbons. J Hazard Mater 431:128548. https://doi.org/10.1016/j.jhazmat.2022.128548

[33] Mun C, Ehrhardt JJ, Lambert J, Madic C (2007) XPS Investigations of Ruthenium Deposited onto Representative Inner Surfaces of Nuclear Reactor Containment Buildings. Appl Surf Sci 253:7613-7621. https://doi.org/10.1016/j.apsusc.2007.03.071

[34] Trovarelli A (1996) Catalytic Properties of Ceria and CeO_2-Containing Materials. Catal Rev 38(4):439-520. https://doi.org/10.1080/01614949608006464

[35] Shearer GC, Chavan S, Bordiga S, Svelle S, Olsbye U, Lillerud KP (2016) Defect Engineering: Tuning the Porosity and Composition of the Metal–Organic Framework UiO-66 via Modulated Synthesis. Chem Mater 28(11):3749–3761. https://doi.org/10.1021/acs.chemmater.6b00602

[36] Bambalaza SE, Langmi HW, Mokaya R, Musyoka NM, Khotseng LE (2020) Experimental Demonstration of Dynamic Temperature-Dependent Behavior of UiO-66 Metal–Organic Framework: Compaction of Hydroxylated and Dehydroxylated Forms of UiO-66 for High-Pressure Hydrogen Storage. ACS Appl Mater Interfaces 12(22):24883–24894. https://doi.org/10.1021/acsami.0c06080

[37] Peterson GW, Mahle JJ, DeCoste JB, Gordon WO, Rossin JA (2016) Extraordinary NO_2 Removal by the Metal–Organic Framework UiO-66-NH_2. Angew Chem Int Ed 55:6235–6238. https://doi.org/10.1002/anie.201601782

[38] Ebrahim AM, Levasseur B, Bandosz TJ (2013) Interactions of NO_2 with Zr-based MOF: Effects of the size of organic linkers on NO_2 adsorption at ambient conditions. Langmuir 29(1):168-1748. https://doi.org/10.1021/la302869m

[39] McKeown DA, Hagans PL, Carette LPL, Russell AE, Swider KE, Rolison DR (1999) Structure of Hydrous Ruthenium Oxides: Implications for Charge Storage. J Phys Chem B 103:4825-4832. https://doi.org/10.1021/jp990096n